U. SHEIKH et al.

MULTI-MACHINE STUDIES OF LOW-Z BENIGN TERMINATION OF RUNAWAY ELECTRON BEAMS AND EXTRAPOLATION TO ITER

U. SHEIKH, A. BATTEY, J. DECKER, M. KONG, M. PEDRINI, H. REIMERDES, L. SIMONS, E. TONELLO, C. WANG

EPFL, Swiss Plasma Center (SPC), CH – 1015 Lausanne, Switzerland

Email: umar.sheikh@epfl.ch

V. BANDARU

Indian Institute of Technology Guwahati, Guwahati, Assam, India

O. FICKER J. CALOUD

Institute of Plasma Physics of the CAS, Prague, Czech Republic

C. PAZ-SOLDAN

Department of Applied Physics and Applied Mathematics, Columbia University, New York, NY 10027, USA

E. NARDON, C. REUX, N. SCHOONHEERE, L. SINGH

CEA, IRFM, F-13108 St-Paul-Lez-Durance, France

H. BERGSTROM, P. HEINRICH, M. HOELZL, G. PAPP, B. SIEGLIN

Max-Planck-Institut für Plasmaphysik, Boltzmannstr. 2, 85748 Garching, Germany

M. HOPPE

Department of Electrical Engineering, KTH Royal Institute of Technology, Stockholm, Sweden

E. HOLLMANN

University of California—San Diego, La Jolla, CA 92093, United States of America

S. JACHMICH

ITER Organization, Route de Vinon-sur-Verdon - CS 90 046, 13067 St Paul Lez Durance Cedex, France

C. LIU

Physics Department, Peking University, Beijing, China

THE ASDEX UPGRADE TEAM 1 , JET CONTRIBUTORS 2 , THE TCV TEAM 3 , THE DIII-D TEAM AND THE WPTE TEAM 4

- ¹ See the author list of H. Zohm et al., Nucl. Fusion 64 112001 (2024)
- ² See author list of J. Mailloux et al., Nucl. Fusion 62 042026 (2022)
- ³ See author list of B. Duval et al,. Nucl. Fusion 64 112023 (2024)
- ⁴ See the author list of E. Joffrin et al Nucl. Fusion 64 112019 (2024)

Abstract

Tokamak disruptions present a major challenge to fusion devices, potentially generating highly damaging runaway electron (RE) beams. This paper investigates a novel mitigation strategy, low-Z benign termination, which uses low-Z material injection to trigger a current-driven magnetohydrodynamic (MHD) instability that deconfines and disperses the RE beam. A multi-machine experimental campaign on AUG, COMPASS, DIII-D, JET, and TCV established a two-step process: recombination of the companion plasma by low-Z neutrals followed by a rapid MHD collapse. We systematically map the operational boundaries of this process, identifying a critical neutral pressure window for successful termination. To understand and extrapolate these results to ITER, we utilize a multi-code modeling approach. SOLPS-ITER simulations successfully replicate the experimental recombination phase, validating that neutral conduction, rather than radiation, is the dominant energy loss mechanism. JOREK and M3D-C1 simulations of the final MHD collapse show that lower plasma density and higher resistivity increase mode growth rates, consistent with experimental observations. This work provides a comprehensive framework for optimizing and ensuring the reliability of benign termination as a critical RE mitigation strategy for future devices

1. INTRODUCTION

Tokamak disruptions pose a significant threat to fusion devices, potentially causing severe thermal and electromagnetic damage to the vessel and its components. To mitigate these effects, massive material injection (MMI) is often used to disperse the plasma's energy over a larger area by enhancing radiation. While high- and

medium-Z materials are effective for this purpose due to their high radiative efficiency, they can inadvertently lead to the formation of a runaway electron (RE) beam.

This occurs because MMI of these materials causes a sudden increase in plasma resistivity, generating a strong electric field that can accelerate electrons to relativistic energies. If this accelerating force overcomes the collisional drag, a powerful RE beam forms. On a large-scale device like ITER, an unmitigated RE beam could cause severe damage, including deep melting of plasma-facing components and failure of cooling channels. Due to the high likelihood of RE beam formation during disruptions on ITER [1], a robust strategy for their mitigation is essential as the final line of defense.

1.1 A NEW APPROACH FOR REMITIGATION

Previously explored methods for mitigating a fully formed RE beam, such as high-Z MMI, have had limited success and are not predicted to be sufficient for ITER's high currents and expected avalanche gains [2]. This has led to the development of a novel strategy known as 'low-Z benign termination' [2, 3]. This technique utilizes the injection of low-Z, hydrogenic materials and a reduction in edge safety factor (qedge) to trigger a current-driven kink instability, which effectively spreads the energy of the RE beam. This process significantly reduces the localized heat fluxes, preventing the type of damage that unmitigated RE beams can cause. Since the initial demonstrations on the DIII-D and JET tokamaks in 2021 [2, 3], the community has been exploring the operational boundaries to understand the underlying physics, which are not yet fully clear [4]. This work aims to systematically investigate and establish the benign termination boundary across a range of devices—AUG, COMPASS, DIII-D, JET, and TCV— and compare with modelling in order to develop a reliable framework for its extrapolation and eventual implementation on ITER.

1.2 BENIGN TERMINATION SCENARIO

RE beam generation on AUG, COMPASS, DIII-D, JET and TCV is achieved through MMI of impurities [5, 6, 7]. The RE benign termination process itself consists of two critical steps, which have now been validated across all devices. The first step is the recombination of the companion plasma via low-Z (D or H) injection. Experiments have confirmed that recombination is a function of achieved neutral pressure and not the injection method (massive gas injection (MGI), shattered pellet injection (SPI), or fueling valves). A key finding is that recombination is driven by neutral gas conduction, not radiative cooling, as indicated by a decrease in radiated power [4].

The second step is the reduction of the q_{edge} to trigger an MHD instability that expels the REs in microsecond timescales. This has been achieved via multiple techniques: plasma compression on the center column, vertical displacement, and current or toroidal field ramps [3, 4]. Crucially, the final termination was found to be agnostic to the method used to achieve a low q_{edge} , with all paths resulting in a rapid current quench and a large HXR burst signifying RE loss. While the specific q_{edge} threshold for instability varied (2-3 on AUG/DIII-D/TCV, higher on JET), the core physics remained consistent across machines. The operational limits of this process, particularly the role of neutral pressure, are explored in the following section.

2. OPERATIONAL LIMITS

Approaches to low q_{edge} via plasma compression at varying densities, controlled by neutral pressure, were conducted on AUG, DIII-D, JET and TCV. These experiments explored the transition from a benign to a non-benign termination. On all four machines, an increase in companion plasma electron density (n_e) was found to reduce the wetted area and increase the maximum tile temperature. This is attributed to a decrease in Alfvénic velocity with increasing n_e , resulting in slower mode growth [4]. At RE currents above 1 MA on JET, this trend was not as distinct because regeneration of REs began to occur [8].

The minimum pressure required to achieve recombination was found to be a factor of RE current density and impurity density in the vacuum vessel, as shown in Fig. 1a. All of the pulses presented in this Fig. are the results of a primary Ar injection and a secondary D injection, with the exception of the filled green circles that indicate a primary injection of Ne on TCV. This comparison is critical as ITER will use Ne in the disruption mitigation system and most current machines require Ar to generate RE beams. It was found that there was no significant difference in required neutral pressure for recombination between Ar and Ne across the large range explored.

The expected ITER impurity and current density range, shown by the cyan line, is based on the foreseen SPI neon injection of $4x10^{21}$ - $5x10^{22}$ atoms into the $1080m^3$ vessel volume. The RE current density (400- $1200kA/m^2$) is based on a 5-15MA range with a minor radius of 2m. A lower RE current is possible but would likely lead to a smaller plasma, and thus similar RE current density. Studies comparing D and H as the secondary

U. SHEIKH et al.

injection have also been presented and the difference was found to be negligible for the minimum recombination pressure requirement [4].

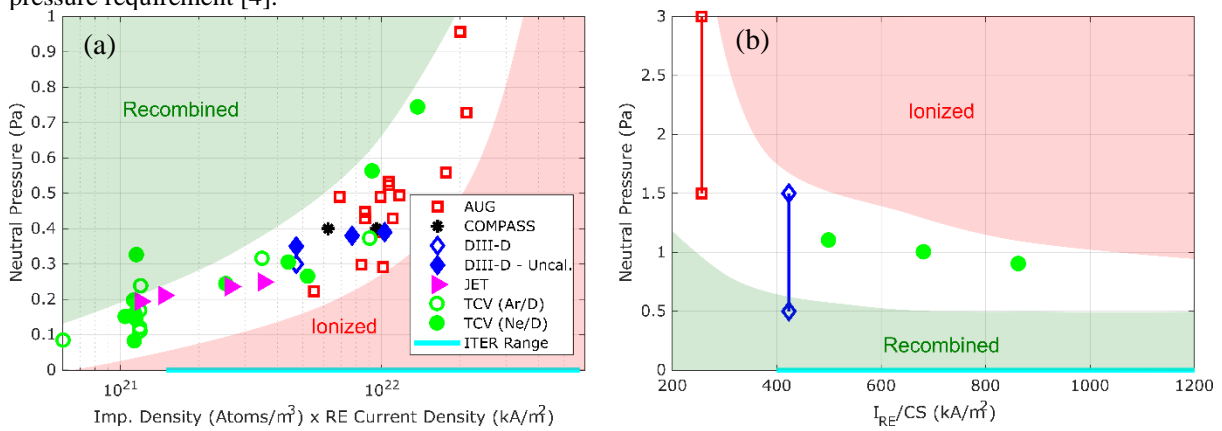


Figure 1 – Multimachine database for the neutral pressure required to achieve recombination of the companion plasma (a) as a function of RE current and impurity density. (b) the neutral pressure at which an n_e rise is observed as pressure is increased further as a function of RE density. The expected ITER range is indicated by the cyan on the x-axis.

Neutral pressures above ~1Pa revealed a decrease in wetted area on TCV, reducing the efficacy of the benign termination due to an increase in n_e from RE-neutral collisions [9]. This hypothesis is supported by a measured decrease in electron temperature (T_e) as the n_e increases [4]. Controlled scans of neutral pressures were also carried out on AUG and DIII-D, producing n_e increases between 0.5-3Pa, as shown in Fig. 1b. Experiments on TCV reported that the measured increase in n_e at high neutral pressures did not vary significantly with injected impurity quantity, but was sensitive to increases in RE current density. Furthermore, it was noted on AUG and TCV that the increase in n_e at high pressure was not as sharp compared to the recombination limit at low pressure [4].

The experimental results presented in this section indicate that the neutral pressure required to achieve recombination on ITER will be in the range of 0.2-0.8Pa. These results also suggest that the companion plasma n_e will increase again above 1-1.5Pa at an RE current density of 400-1200 kA/m². This poses a significant challenge for ITER as the expected vessel pressure is ~30Pa with 2.1×10^{25} atoms for a staggered injection scheme into a 15MA H-mode plasma [10]. Whilst this upper pressure limit will ease as the beam current density decays due to decreased collisionality between the REs and the neutrals, it is likely the staggered mitigation scheme will need to be optimized given this constraint for RE benign termination.

3. MODELLING OF OPERATIONAL LIMITS

The experimental campaign has provided a wealth of data on the low-Z benign termination scheme, but a comprehensive theoretical understanding requires advanced numerical modelling to interpret the results and extrapolate to ITER. The complexities of this process, which involve intricate interactions between the companion plasma, REs, and injected neutrals, cannot be fully captured by a single model. Therefore, this section presents a multi-code approach to simulate the key phases of benign termination.

The modelling effort is split into two parts, each addressing a distinct physical process. The first part uses the SOLPS-ITER code to model the steady-state phase of the termination, focusing on the crucial recombination of the companion plasma. These simulations provide a detailed look into the particle, momentum, and energy balance governed by the interaction between the plasma and injected neutrals. The second part includes results from both JOREK and M3D-C1 codes, and focuses on the final, fast MHD collapse of the RE beam. This work aims to pinpoint the critical parameters—such as n_e , plasma resistivity, and RE current—that influence the growth and evolution of the MHD instabilities responsible for the successful termination.

3.1 RECOMBINATION PRESSURE REQUIREMENT

SOLPS-ITER is a widely used tool for edge and divertor plasma physics, coupling a fluid description for electrons and ions with a kinetic Monte Carlo treatment of neutrals [11, 12]. The code solves particle, momentum and energy conservation for each species on a 2D poloidal plane, assuming a fixed magnetic equilibrium and toroidal symmetry. It incorporates a wide range of plasma-neutral collision processes, including impurities as independent neutrals and ion populations. For the first time, SOLPS-ITER was used to model the steady-state phase of benign termination experiments in TCV. These simulations provide detailed insights into particle, momentum and energy balance between the thermal companion plasma and the injected neutrals. The Ohmic heating from the RE current, sustaining the companion plasma, is modelled as an imposed energy source for the

thermal electron population (Fig. 2a). Simulations were performed for both D and H plasmas with impurities neglected in this first study. Neutral pressure was varied by changing the gas fueling rate in the simulations, while the electron input power was kept fixed.

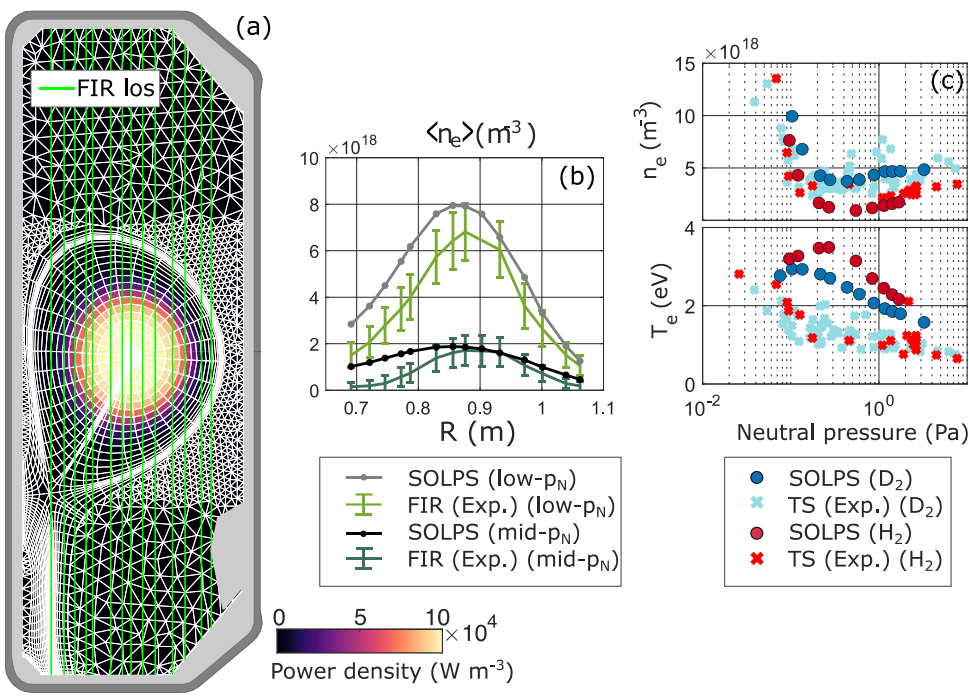


Figure 2 (a) SOLPS-ITER mesh and input power density distribution used in the simulations. (b) Comparison of the line-integrated n_e from TCV interferometer (FIR) and the synthetic SOLPS line-integrated n_e , for two different neutral pressure values. (c) Simulated (dots) and experimental (crossed) central n_e (top) and T_e (bottom) as a function of neutral pressure, for deuterium and hydrogen plasmas.

Despite the simplifying hypothesis, SOLPS-ITER simulations reproduce the main trends observed in experiments. Fig. 2b shows the radial profiles of the integrated n_e as measured by TCV interferometer (FIR) and modelled by SOLPS. The code accurately reproduces the integrated profiles and absolute values of n_e at different neutral pressures. The results of the full pressure scan are shown in Fig. 2c. n_e (top panel) and T_e (bottom panel) in the proximity of the magnetic axis are plotted as a function of neutral pressure and compared with the experimental values measured by the Thomson Scattering (TS) system at the same location. Neglecting impurities results in a slight overestimation of T_e , due to the unaccounted-for radiated power, while good agreement is found for n_e , recovering the non-monotonic behavior observed in experiments for n_e (p_N). At pressures below ~0.4Pa, the central n_e and T_e decrease with increasing pressure, while the trend reverses at pressures higher than ~0.4Pa. In the high-pressure regime, the code also correctly recovers D2 plasmas (blue in Fig. 2c) being denser than H2 plasmas (red in Fig. 2c) for the same neutral pressure [4].

Energy dissipation of the companion plasma is found to be governed almost entirely by collisions between thermal ions and electrons, and, neutral atoms and molecules. Less than 1% of the input power remains in the plasma or is transported to the wall as plasma fluxes. Instead, the energy is either lost directly by thermal electrons in collisions with neutrals or it is transferred from the electrons to the ions and ultimately from the ions to the neutrals. In steady state, power is lost either through radiation or via neutral conduction to the wall in the form of kinetic energy. In line with reported experiments [4], the latter is the dominant energy sink in these simulations, although radiation might be underestimated due to the absence of impurities.

3.2 IMPACT OF ELECTRON DENSITY AND RESISTIVITY ON FINAL COLLAPSE

3.2.1 TCV Simulations

The final collapse of the RE beam is modelled with the 3D non-linear MHD code JOREK using a reduced MHD model [13]. JOREK contains various extensions, including a fluid description of REs self-consistently coupled with the main plasma, facilitating the modelling of benign termination [14]. The simulations presented are initialised during the compression phase and terminate at the final collapse of the RE beam. During this period, the total plasma current is assumed to be carried by the RE beam and the plasma has contacted the high-field-side (HFS) wall. The RE avalanche source is activated to include RE regeneration in the confined region during the

RE termination. RE parallel advection at the speed of light is mimicked by a parallel diffusivity $D_{//,RE}=10^9 m^2/s$. The initial plasma equilibrium is taken from TCV discharge #86978 at t=1.337ms, where $I_p=I_{RE}=185kA$. Both Ohmic heating and the impurity radiation are turned off, and the core plasma T_e is artificially maintained at experimentally measured values of 3-4eV. The neutrals are not included in this first-stage work to simplify the simulation. Instead, we use the resulting profiles from the SOLPS-ITER simulations and study the influence of n_e and plasma resistivity on the MHD instabilities and the deconfinement of REs, which could be varied by the neutral pressure in the experiment. Two separate scans of n_e and plasma resistivity were conducted.

The n_e scan of n_e =5×10¹⁷ - 2×10¹⁹m⁻³, covers the entire experimental range [4]. The energy growth of the n=1 MHD modes, with all possible m numbers, during the scan is presented in Fig. 3a, where m and n are the poloidal and toroidal harmonic numbers respectively. It should be noted that n=1-5 harmonics were included in the simulations but only the n=1 is presented as the m/n=2/1 mode always dominates. The MHD activity is proven to be highly unstable at this stage, and the mode energy grows from noise to 0.1kJ scale (corresponding to $\delta B/B_{pol}\sim5\%$) within tens of microseconds in most cases. The RE deconfinement occurs in several microseconds (Fig. 3b). As discussed in section 2, lower n_e leads to higher Alfvénic velocity and higher growth rate of MHD modes. The corresponding RE deconfinement thus occurs earlier. However, the expelling of REs is still fast and complete in the high-density limit of the scan despite a slightly slower I_{RE} quench. The evidence of non-benign termination at high n_e is unclear based on present simulation results. An abnormal case was found in the low- n_e limit of n_e =5×10¹⁷m⁻³, where the mode energy saturates at approximately 0.02kJ. The I_{RE} quench thus takes an order of magnitude longer relative to the high- n_e cases because under a lower amplitude of magnetic stochasticity, REs will need to travel over a longer distance before they are lost on the wall (maximum connection length 10^5 m vs 10^4 m under higher densities). More analysis and experimental validation are needed to determine whether this abnormal point at low n_e indicates a low- n_e limit for benign termination.

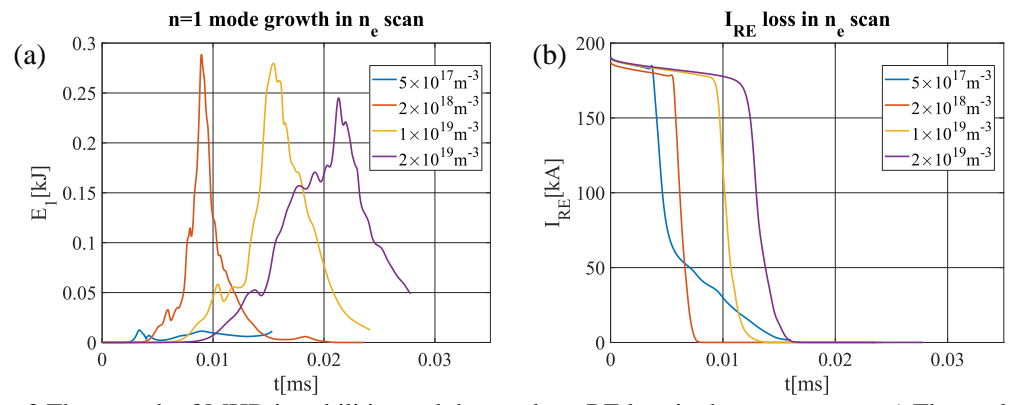


Figure 3 The growth of MHD instabilities and the resultant RE loss in the scan over n_e. a) The evolution of the magnetic energy carried by n=1 modes. b) Decay of total RE current.

A second scan of the Spitzer resistivity ($\eta_{Spitzer}$) by a factor of 0.1, 0.3, 1, 3, and 10 while keeping the core T_e around 3eV and n_e =2×10¹⁸m⁻³was carried out. The mode growth rates match qualitatively with the resistive mode theory [15], where they grow faster under higher η (Fig. 4a). Under low resistivity ($\eta = 0.3 \times$, 0.1× $\eta_{Spitzer}$), the collapse of I_{RE} occurs only slightly later than in the higher resistivity cases (Fig. 4b), but an I_{RE} plateau survives after the first collapse because of the lower level of magnetic stochasticity and thus RE loss. The slower termination of the RE plateau here indicates a higher risk of a non-benign termination.

In summary, the preliminary JOREK scans of n_e and $\eta_{Spitzer}$ show a trend that matches qualitatively with the theory on resistive MHD modes, where the mode growth rates increase under lower n_e and higher resistivity. However, it is difficult to quantitatively compare the MHD activity and the RE loss rate with the experimental data. More comparable data would be the thermal load to the wall, which is also the straightforward criterion for a benign termination. In the following work, the RE energy deposition on the wall will be modelled via particle tracing in the present simulation results [16]. This result will be compared with the infrared camera and thermocouple data from the TCV experiments. Another uncertainty comes from the parallel transport model of the RE fluid model. The diffusion model with $D_{//,RE}$ =109m²/s gives slower RE transport than advection at the speed of light. A faithful advection model or a higher $D_{//,RE}$ would require many more CPU hours. The value we use is expected to be appropriate to capture the RE transport in a sufficiently stochastic magnetic field, as long as the typical timescale of RE loss is not larger than that of MHD activities [16], which is the case in our simulations. However, the validity of the RE-MHD interaction in this model still needs to be benchmarked with the kinetic RE model. Further simulations will also incorporate the diffusive neutral equation in JOREK and consider the RE-impact ionization of neutrals, which is crucial for investigating the upper limit of neutral pressure for a benign termination.

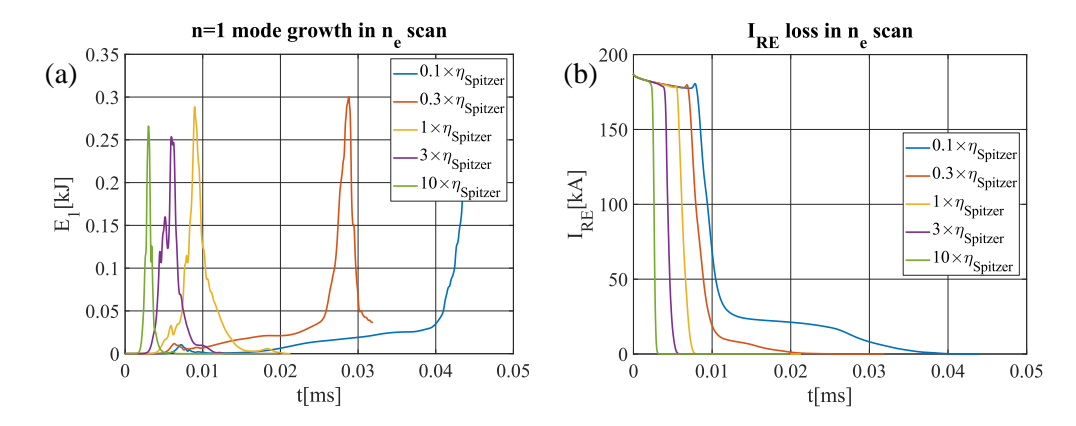


Figure 4 The growth of MHD instabilities and the resultant RE loss in the scan over resistivity. a) The evolution of the magnetic energy carried by n=1 modes. b) Decay of total RE current.

3.2.2 AUG Simulations

Modeling of the AUG experimental cases with JOREK has been done with discharges #41326 and #40891, which correspond to benign and non-benign termination experiments [4]. The starting equilibrium for the 3D simulations correspond to the plasma state in the RE plateau phase just before the RE beam current crash, with I_p = I_{RE} =200kA, q_{axis} =1.13, q_{95} =2.2, n_{Ar} =1.11x10²⁰m⁻³ and n_D =1x10²⁰ m⁻³, where n_D is the total Deuterium particle density including neutrals. The coronal equilibrium model is used to obtain the charge-state distribution of the Argon impurities. Spatially uniform densities (Ar and D) are used and the thermal evolution of the plasma is frozen for simplicity. Sensitivity with respect to the T_e of the plasma are being investigated using three different T_e of 2eV, 1eV and 0.95eV. It must be noted that the ionization fraction of the plasma reduces by about an order of magnitude each as the T_e decreases from 2eV to 1eV, and from 1eV to 0.95eV. Furthermore, even at the lowest T_e considered, the Alfvén velocity is still about two orders of magnitude smaller than the speed of light. The RE fluid model [17] in JOREK is used to model the transport of REs with an ExB drift advection and RE parallel diffusion D_{ILRE} =1.55x10⁹ m²/s used to mimic the fast parallel advection of REs at the speed of light.

Simulations show that perturbing the RE plateau-phase equilibrium leads to a prompt exponential growth of the m/n=2/1 tearing mode close to the plasma edge. Furthermore, it is observed that the linear growth rate of the mode increases substantially as the plasma T_e decreases. Such a faster growth rate is attributed both to the increased resistivity as well as the depletion of ion-density, at lower plasma T_e . However, the increase in linear growth rates at lower T_e are not observed to scale as per the theoretical estimate for a resistive tearing mode. The linear growth rates of the m/n=2/1 mode at T_e =1eV and T_e =0.95eV were around 60% and 81% more respectively than that at T_e =2eV.

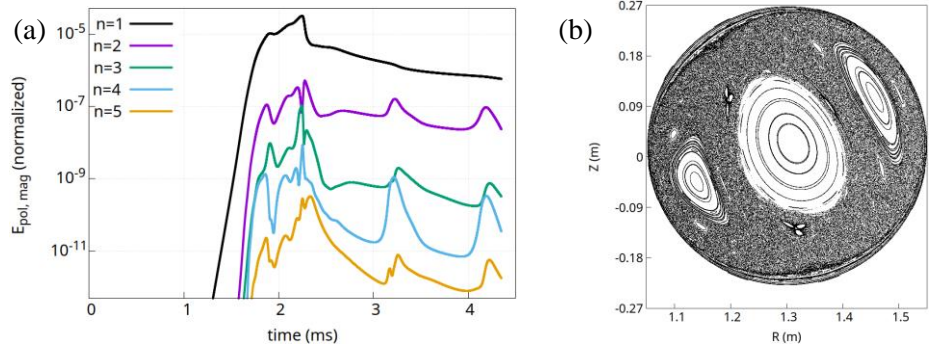


Figure 5 - a) Evolution of magnetic energies of different toroidal modes; b) Poincare plot showing magnetic stochastization at peak mode energy of n=1, at t=2.26ms (both for the $T_e=2eV$ case)

Significant growth of the dominant m/n=2/1 mode is followed by a sequential destabilization of the higher toroidal modes (n=2, 3, 4 and 5), and an eventual non-linear saturation of the mode energies at about 0.5% of the equilibrium poloidal magnetic energy. For the 2eV case, stochastization of the magnetic field ensues which triggers a drop of RE current due to parallel transport (see Fig. 5). However, the flux-surfaces near the plasma edge are observed to heal at a timescale of ~0.5ms, which does not allow a fast loss (or crash) of the RE beam current. An RE current loss of around 15% is observed in the 2eV case over a duration of around 2.6ms. The lower T_e simulations (ongoing) are expected to yield a faster and larger crash of the RE beam current. Further

studies are ongoing currently to improve the simulations to better mimic the conditions in the experiment (e.g. with respect to magnetic boundary conditions, q_{95} etc.), which will be reported in the future.

3.3 RE CURRENT DENSITY SCALING

The extended-MHD code M3D-C1 was employed to simulate the excitation of MHD instabilities during the final termination event in AUG. Similar to JOREK, M3D-C1 can model current-driven MHD modes in the presence of strong RE current, by utilizing a fluid-based RE current description. The coupling of RE current to the MHD is enabled through an additional term in Ohm's law. More details of the RE fluid model in M3D-C1 are available in [17, 18]

A scan of runaway RE current for the benign termination scheme was performed in AUG. In discharges 40891, 42922, 40893, and 40895, the plateau RE current prior to the final termination was approximately 200, 400, 500, and 600kA [4]. Analysis of the total plasma current, safety factor q_a , and magnetic axis location shows that, in all four cases, the final termination was triggered by plasma contraction as q_a dropped to near 2. This indicates that the dominant MHD instability responsible for the termination was the m/n=2/1 mode, consistent with observations from benign termination experiments in DIII-D [3].

Based on these conditions, MHD equilibria were reconstructed for the four cases and subsequently used as inputs to the M3D-C1 simulations. The plasma pressure was taken to be negligible (with β <0.1%), and the safety factor q profile was prescribed as quadratic with q_0 =1.1 and q_a =2.05. The halo plasma was modeled with a circular cross-section, bounded on the inboard side at R=1.0633m and Z=0. For each case, the magnetic axis location was adjusted to satisfy the constraint of the total plasma current.

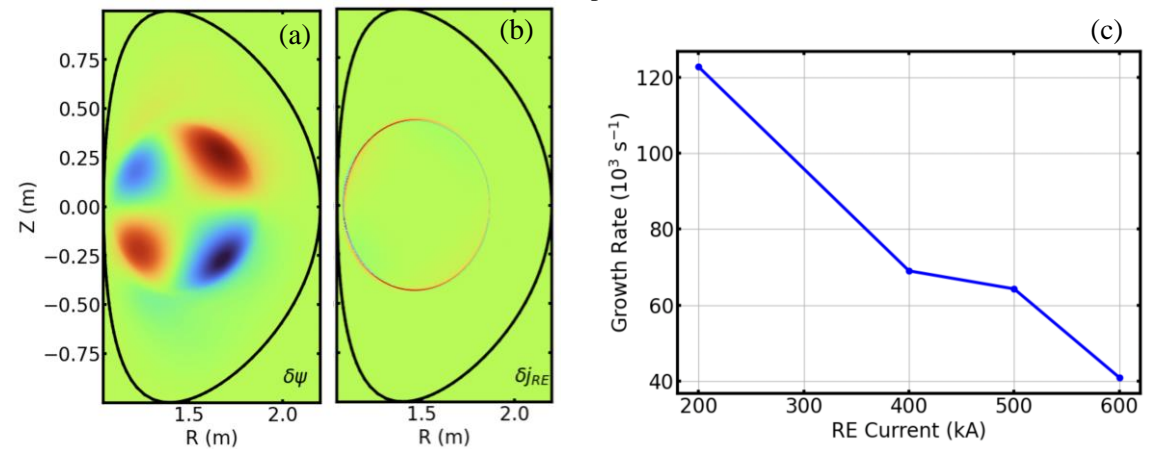


Figure 6: Mode structure of resistive kink mode for I_{RE} =600kA (a and b). Growth rate of m/n=2/1 resistive kink mode for different RE plateau current (c)

We first carried out linear MHD simulations for n=1 mode only, assuming that the total plasma current was initially carried entirely by REs. In all four cases, the unstable (2,1) mode was clearly identified. Figs. 6a and b illustrate the mode structure of the perturbed poloidal flux ($\delta\psi$) and perturbed RE current (δj_{RE}) for the 600kA case. The perturbed RE current is strongly localized near the q=2 surface, which is close to the plasma boundary. We further compared the linear mode growth rates across the four cases, as shown in Fig. 6c. The results indicate that the growth rate decreases as the RE current increases from 200kA to 600kA. This trend suggests that the benign termination strategy, which relies on the excitation of strong MHD modes, may become less effective in devices operating at higher currents. However, the linear growth rate is highly sensitive to the q_{edge} , which evolves rapidly during plasma contraction. Consequently, the influence of total current on the growth rate may not play a dominant role in determining the eventual mode amplitude. Nonetheless, estimates suggest that within 0.1ms, the instability can reach amplitudes sufficient to induce strong magnetic stochasticity and significant RE transport. A detailed investigation of this process, including the dependence of RE loss on the plateau current, requires nonlinear simulations of the final termination stage, which will be addressed in future work.

4. CONCLUSIONS

This paper successfully synthesizes multi-machine experimental results and advanced modeling to develop a reliable framework for low-Z benign termination of runaway electron (RE) beams, a critical mitigation strategy for ITER. The research confirms a robust two-step process: first, the recombination of the companion plasma via low-Z material injection (D or H), driven by neutral gas conduction, and second, a current-driven

MHD instability triggered by a low q_{edge}. Experiments across AUG, COMPASS, DIII-D, JET, and TCV established a key operational window for this process, finding that the required neutral pressure for recombination scales with RE current density, with an optimal range for ITER estimated at 0.2–0.8Pa. The studies also revealed a significant challenge: at pressures above ~1.5Pa, the companion plasma n_e rises again due to RE-neutral collisions, which could make the termination less effective.

Advanced multi-code simulations with SOLPS-ITER, JOREK, and M3D-C1 explored the physics of these experimental findings. The SOLPS-ITER model accurately reproduced n_e and T_e trends, confirming neutral conduction as the dominant energy sink. JOREK and M3D-C1 simulations of the final MHD collapse showed that lower n_e and higher resistivity lead to faster mode growth, supporting experimental observations. The modeling also identified a potential risk at low resistivity, where a dangerous RE plateau can survive after the initial collapse. A comparison between JOREK simulations of TCV and AUG discharges highlights the need for comprehensive models that include full experimental conditions. While TCV simulations showed faster mode growth with lower n_e , AUG simulations demonstrated that a lower plasma T_e (increasing resistivity) also substantially increases the linear growth rate of the dominant m/n=2/1 mode, even with the presence of impurities. This interplay between n_e and resistivity underscores the need for more comprehensive modeling that can capture the full suite of experimental parameters, including the evolution into the unstable state phase and effects beyond the RE fluid model [20]. This work provides a high-fidelity starting point to understand and optimize the low-Z benign termination scheme for ITER.

ACKNOWLEDGEMENTS

This work has been carried out within the framework of the EUROfusion Consortium, partially funded by the European Union via the Euratom Research and Training Programme (Grant Agreement No 101052200—EUROfusion). The Swiss contribution to this work has been funded by the Swiss State Secretariat for Education, Research and Innovation (SERI). This work was supported in part by the Swiss National Science Foundation. Views and opinions expressed are however those of the author(s) only and do not necessarily reflect those of the European Union, the European Commission or SERI. Neither the European Union nor the European Commission nor SERI can be held responsible for them. This material is based upon work supported by the U.S. Department of Energy, Office of Science, Office of Fusion Energy Sciences, using the DIII-D National Fusion Facility, a DOE Office of Science user facility, under Awards DE-FC02-04ER54698, DE-FG02-07ER54917, and DE-SC0022270.

Disclaimer: This report was prepared as an account of work sponsored by an agency of the United States Government. Neither the United States Government nor any agency thereof, nor any of their employees, makes any warranty, express or implied, or assumes any legal liability or responsibility for the accuracy, completeness, or usefulness of any information, apparatus, product, or process disclosed, or represents that its use would not infringe privately owned rights. Reference herein to any specific commercial product, process, or service by trade name, trademark, manufacturer, or otherwise does not necessarily constitute or imply its endorsement, recommendation, or favoring by the United States Government or any agency thereof. The views and opinions of authors expressed herein do not necessarily state or reflect those of the United States Government or any agency thereof.

REFERENCES

- [1] Vallhagen, O., et al. Nuclear Fusion 62.11 (2022): 112004
- [2] Reux, C., et al. Physical Review Letters 126.17 (2021): 175001.
- [3] Paz-Soldan, C., et al. Nuclear Fusion 61.11 (2021): 116058
- [4] Sheikh, Umar, et al. Plasma Physics and Controlled Fusion 66.3 (2024): 035003.
- [5] Decker, J., et al. Nuclear Fusion 62.7 (2022): 076038.
- [6] Pautasso, G., et al. Plasma Physics and Controlled Fusion 59.1 (2016): 014046.
- [7] Reux, C., et al. Nuclear Fusion 55.9 (2015): 093013.
- [8] Reux, C., et al. 50th EPS Conference on Plasma Physics (EPS 2024), Salamanca, Spain, 2024.
- [9] Hoppe, M., et al. Plasma Physics and Controlled Fusion 67.4 (2025): 045015.
- [10] Sheikh, U., et al. "Pellet Size Optimization for the ITER SPI." Third Technical Meeting on Plasma Disruptions and their Mitigation. Presentations. No. INIS-XA--24M3135. 2024.
- [11] S. WIESEN et al. Journal of Nuclear Materials, 463:480–484, August 2015.
- [12] X. BONNIN et al. Plasma and Fusion Research, 11(0):1403102–1403102, 2016.
- [13] Hoelzl, M., et al. Nucl. Fusion 64 112016 (2024)
- [14] Bandaru, V., et al. Phys. Rev. E 99, 063317 (2019)
- [15] Graves, J. P., et al. Plasma Phys. Control. Fusion 64 014001 (2022)
- [16] Bandaru, V., et al. Nuclear Fusion 64 076053 (2024)
- [17] Bandaru, V., et al. Phys. Plasmas 31 082503 (2024)
- [18] Liu, C., et al. Plasma Phys. Control. Fusion 63 125031 (2021)
- [19] Zhao, C., et al. Nucl. Fusion 60 126017 (2020)
- [20] Bergström, H., et al. Plasma Physics and Controlled Fusion 67.3 (2025): 035004.